EBioMedicine 59 (2020) 102892

Contents lists available at ScienceDirect

EBioMedicine

journal homepage: www.elsevier.com/locate/ebiom

Research paper

CHRFAM7A: A human specific fusion gene, accounts for the translational gap for cholinergic strategies in Alzheimer's disease

Kinga Szigeti[a,*], Ivanna Ihnatovych[a], Barbara Birkaya[a], Ziqiang Chen[a], Aya Ouf[a], Dinesh C. Indurthi[a], Jonathan E. Bard[a], Julien Kann[a], Alexandrea Adams[a], Lee Chaves[a], Norbert Sule[b], Joan S. Reisch[c], Valory Pavlik[d], Ralph H.B. Benedict[a], Anthony Auerbach[a], Gregory Wilding[a]

[a] State University of New York at Buffalo, 875 Ellicott St., Buffalo, NY, 14203, USA
[b] Roswell Park Comprehensive Cancer Center, 665 Elm St, Buffalo, NY 14203, USA
[c] UT Southwestern, 5323 Harry Hines Boulevard, Dallas, TX 75390, USA
[d] Baylor College of Medicine, 1 Baylor Plz, Houston, TX 77030, USA

ARTICLE INFO

Article History:
Received 10 February 2020
Revised 11 June 2020
Accepted 29 June 2020

Keywords:
Alzheimer's disease
Pharmacogenetic
α7 nAChR
CHRFAM7A
iPSC

ABSTRACT

Background: Cholinergic neuronal loss is one of the hallmarks of AD related neurodegeneration; however, preclinical promise of α7 nAChR drugs failed to translate into humans. *CHRFAM7A*, a uniquely human fusion gene, is a negative regulator of α7 nAChR and was unaccounted for in preclinical models.
Methods: Molecular methods: Function of *CHRFAM7A* alleles was studied *in vitro* in two disease relevant phenotypic readouts: electrophysiology and Aβ uptake. Genome edited human induced pluripotent stem cells (iPSC) were used as a model system with the human context. Double blind pharmacogenetic study: We performed double-blind pharmacogenetic analysis on the effect of AChEI therapy based on *CHRFAM7A* carrier status in two paradigms: response to drug initiation and DMT effect. Mini Mental Status Examination (MMSE) was used as outcome measure. Change in MMSE score from baseline was compared by 2-tailed T-test. Longitudinal analysis of clinical outcome (MMSE) was performed using a fitted general linear model, based on an assumed autoregressive covariance structure. Model independent variables included age, sex, and medication regimen at the time of the first utilized outcome measure (AChEI alone or AChEI plus memantine), APOE4 carrier status (0, 1 or 2 alleles as categorical variables) and CHRFAM7A genotype.
Findings: The direct and inverted alleles have distinct phenotypes. Functional *CHRFAM7A* allele classifies the population as 25% non-carriers and 75% carriers. Induced pluripotent stem cell (iPSC) models α7 nAChR mediated Aβ neurotoxicity. Pharmacological readout translates into both first exposure ($p = 0.037$) and disease modifying effect ($p = 0.0048$) in two double blind pharmacogenetic studies.
Interpretation: CHRFAM7A accounts for the translational gap in cholinergic strategies in AD. Clinical trials not accounting for this uniquely human genetic factor may have rejected drug candidates that would benefit 25% of AD. Reanalyses of the completed trials using this pharmacogenetic paradigm may identify effective therapy.
Funding:

1. Introduction

Cholinergic neuronal loss is the hallmark of AD related neurodegeneration. Among the nicotinic acetylcholine receptors (nAChR), α7 has been hypothesized to account for the selective neuronal vulnerability in early AD. Consequently, α7 nAChR has been an active drug target for decades [1,2]. Preclinical promise of α7 nAChR agonists and allosteric modulators in animal models failed to translate into humans [3] and frequently contradicting results emerged in the human context. *CHRFAM7A*, a human specific fusion gene between *CHRNA7* and *ULK4* [4], is a putative negative regulator of the α7 nAChR [5,6]. We hypothesized that CHRFAM7A may contribute to the preclinical to clinical translational gap in α7 nAChR targeting therapy.

CHRFAM7A evolved as a result of a series of recombination events including duplications, deletion and inversion in the humanoids [4,7]. Three distinct alleles emerged: the ancestral allele lacking the

* Corresponding author.
E-mail address: szigeti@buffalo.edu (K. Szigeti).

https://doi.org/10.1016/j.ebiom.2020.102892

Research in context

Evidence before this study

α7 nAChR has been implicated in Alzheimer's disease for decades. Extensive basic science, pharmacological preclinical and clinical studies have been performed. At the time of human translation, virtually all drugs that were effective in mice have demonstrated lack of efficacy in humans, underscoring a robust translational gap. *CHRFAM7A*, a uniquely human fusion gene, was discovered in 1998 as an example of human specific fusion genes that have occurred since the human-chimpanzee divergence. CHRFAM7A functional studies are sparse, and are lacking with the human context. CHRFAM7A gets incorporated into the α7 nAChR pentamer and changes its phenotype.

Added value of this study

We demonstrate functional readouts for the *CHRFAM7A* alleles for two phenotypic readouts. For these readouts the inverted allele is a null. This functional genetic knowledge is the key for human translation, as it splits the population 1:3 for non-carriers to carriers of the functional direct allele. To demonstrate the translational gap, we performed two double blind pharmacogenetic studies for both first exposure and disease modifying effect.

Implications of all the available evidence

This is the first proof of concept study that genotype and mechanism specific treatment is feasible in AD. *CHRFAM7A* non carriers, 25% of the AD population accounting for approximately 1.5 million people with AD in the US, could benefit from α7 nAChR selective drugs. Several compounds have been studied extensively in phase 1 and 2 clinical trials, with valuable data to support and accelerate α7 nAChR targeting drug development. Those efforts need to be continued with trial design incorporating *CHRFAM7A* pharmacogenetics. More broadly, FDA approved AChEI drugs may have a DMT effect in non-carriers and need to be tested in preclinical AD and aMCI. The neuronal toxicity data suggests that non-carriers are more sensitive to Aβ, thus agents that reduce amyloid burden could be effective in non-carriers. Future basic science experiments that characterize the function of CHRFAM7A in the human context may results in novel targetable pathways for AD based on the endophenotype. As α7 nAChR is implicated in a broad range of biological processes and diseases including cognition, memory, schizophrenia, systemic inflammation, sepsis and chronic pain, mechanistic insights into CHRFAM7A function will have an impact on all of these diseases.

fusion gene (0 copy), the fusion gene in direct orientation (*CHRFAM7A*), and the fusion gene in inverted orientation characterized by a 2 bp deletion in exon 6 (*CHRFAM7A*Δ2 bp) [7]. The inverted gene is expressed at the RNA level [8], but protein prediction algorithms suggest that translation is unlikely due to Kozak fragment length [7]. CHRFAM7A gets incorporated into the α7 nAChR homopentamer based on gene dosage [9,10] and functions as a dominant negative modulator [5,6]. We previously showed that CHRFAM7A decreases α7 nAChR channel open probability and mitigates Aβ_{1-42} uptake beyond physiological concentrations [11]. Recent data suggests that CHRFAM7A may have a role in the cholinergic anti-inflammatory pathway [12]. In this study we asked the question how CHRFAM7A and CHRFAM7AΔ2 bp modify receptor pentamer function in the human context and whether this could account for the translational gap in α7 nAChR targeting, and more broadly in cholinergic therapies. We used human induced pluripotent stem cells (iPSC) as a model system and translated the readout into human clinical data using double blind pharmacogenetic study design.

2. Materials and methods

Detailed methods are described in the supplementary information.

2.1. Ethical statement, skin biopsy and genotyping

The Institutional Review Board approved the study. The informed consents were obtained from the donors. Subjects requiring legally authorized representatives were excluded from the study.

2.2. iPSC cell culture

iPSCs were grown on irradiated mouse embryonic fibroblasts in DMEM/F12-Glutamax medium supplemented with 10% KnockOut Serum Replacement, 1% Non-essential Amino Acids (NEAA), and 0.1% 2-Mercaptoethanol (all Thermo Fisher). Cells were maintained at 37 °C/5% CO_2 and subcultured every 4–6 days using Dispase (Thermo Fisher).

2.3. MGE progenitors differentiation, culture, and transfection

Neuronal differentiation of iPSC towards Medial Ganglionic Eminence (MGE) progenitors was carried out as described previously [13,14]. MGE cell culturing is described in details in Supplementary materials. MGE progenitors were transfected with either pcDNA3.1-CHRFAM7A-mCherry, pcDNA3.1-CHRFAM7ADelta2bp-mCherry (both a gift from Henry Lester (Addgene plasmid # 62,635, Addgene plasmid # 62,638, respectively[15]) or with pcDNA3.3-mCherry (a gift from Derrick Rossi (Addgene plasmid # 26,823 [16],) constructs according to Ma et al. [17].

2.4. HEK 293 cell culture and transfection

Human embryonic kidney (HEK) 293 cells were maintained in Dulbecco's minimal essential medium (DMEM) supplemented with 10% fetal bovine serum and 1% penicillin–streptomycin, pH 7.4. Human α7 nAChRs and CHRFAM7A were expressed in HEK 293 cells by transient transfection ($CaPO_4$ precipitation method) of these cDNA in ratios of 4:1 or 1:4. To aid surface expression of α7, we co-transfected intracellular chaperones Ric-3 (resistance to inhibitors of cholinesterase 3 [18]) and NACHO (transmembrane protein TMEM35A [19]) in 1:1:1 ratio in all experiments.

2.5. Electrophysiology

Whole cell and single-channel currents were recorded in the cell-attached patch configuration as described previously [20] (Supplementary data, Methods). Kinetic analyses of single channel currents were performed by using QuB [21]. Single channel currents were idealized by segmental k-means algorithm (SKM). nPo was estimated by dividing the cumulative open probability by the number of channels in the patch (maximum number of overlaps of open current levels in the data) as follows:

$$Po = \frac{\sum nPo}{n}$$

2.6. Generation of isogenic iPSC lines, electroporation, and colony selection

TALEN-mediated KI of direct *CHRFAM7A* (UB068i_KI) into the AAVS1 safe harbor site of the constitutively expressed gene *PPP1R12C* on chr19 (position 19q13.42) of the 0 copy ancestral line (UB068) was performed. The expression vector (GeneCopoeia (Cat. No.: DC-DON-SH01 - AAVS1 donor vector)) harbours puromycin resistance gene for selection and fluorescent signal (GFP) for visualization. Individual GFP expressing colonies were picked, PCR screened for the insertion, and passaged. Breakpoint specific TaqMan assay and RT-qPCR were used to quantify copy number and expression level of the inserted gene. Whole genome sequencing was performed to confirm transgene insertion and exclude off target mutations.

2.7. Amyloid beta uptake by fluorescent microscopy

Unlabelled and fluorescently labelled Aβ_{1-42} (both from AnaSpec) were reconstituted according to the manufacturer's protocol. The species of Aβ1−42 was confirmed by measuring concentration and absorbance at 280 nm and using Beer's Law (extinction coefficient = absorbance/concentration/path length). We derived the extinction coefficient at 1280M-1 cm-1 corresponding to the 42 amino- acid peptide with MW 4514. Aβ_{1-42} was diluted in 1% NH_4OH and PBS was added to reach the concentration of 1 mg/ml, briefly sonicated and either used immediately or aliquoted and kept at −20 °C.

Amyloid beta uptake was performed using fluorescently labelled Aβ_{1-42} as described previously [22]. Uptake was pathologically characterized by a blinded pathologist and two independent raters for positive cells, grade (no uptake, low grade, high grade) and intensity measured by ImageJ plugin. α7 nAChR mediated endocytosis was characterized by co-localization of CHRNA7, acidic compartment (LysoTracker) and fluorescently labelled Aβ_{1-42} (HiLyteFluor555).

2.8. Flow cytometry

MGE progenitors grown on 12 well plates (400,000 cells/well) were treated with various concentrations of HiLyteFluor 488-Aβ_{1-42} or Aβ_{1-42} HiLyteFluor 555- Aβ_{1-42} (1 nM to 500 nM) for 18 h. The cells were detached with Accutase, pelleted by centrifugation at 200x*g* for 5 min, and washed three times with PBS. Flow cytometry was performed using LSRII-Fortessa with FACS DIVA (BD Biosciences). Data were analysed using FlowJo software (https://www.flowjo.com/).

2.9. ELISA

After Aβ_{1-42} treatment, total cell lysates were collected and stored at −80 °C. Concentration of Aβ_{1-42} in the cell lysates was estimated using a human specific high sensitivity Aβ_{1-42} ELISA kit (Thermo Fisher) according to the manufacturer's protocol.

2.10. Lactate dehydrogenase (LDH) cytotoxicity assay

The LDH assay was carried out according to the manufacturer's protocol. Briefly, MGE progenitors derived from the UB068, UB068_CHRFAM7A, and the UB052 lines were seeded in 96−well plastic plates (20,000 cells/well). The cells were cultured for 24 h prior to treatment with either AChEIs (50 μM donepezil, 50 μM rivastigmine) or a specific α7 nAChR agonist, encenicline (50 μM,) followed by 48 h treatment with Aβ 1−42 (7,5 μM). LDH release was detected spectrophotometrically. Absorbance was measured at 450 nm and 600 nm using BioTek microtiter plate reader.

2.11. ApoTox-Glo Cytotoxicity and Caspase-GLO 3/7 Assay

ApoTox-Glo (Promega) Assay to measure cytotoxicity and caspase activity was done according to the manufacturer's protocol. Live and dead cell protease activities were measured using fluorogenic cell-permeant (live) and cell-impermeant (dead) peptide substrate. Fluorescence was measured at 400Ex/505Em for viability and 485Ex/520Em for Cytotoxicity. Caspase 3/7 activity was measured by luminescence after adding Caspase-Glo 3/7 reagent to all wells.

2.12. Study cohorts

The University at Buffalo Alzheimer's Disease and Memory Disorders Center clinical research cohort is an observational study with genetic component [23,24]. Inclusion criteria included consensus diagnosis of aMCI or AD, documentation of time of initiation of AChEI therapy, baseline MMSE within 3 months prior to AChEI initiation, at least 1 follow up assessment within 3−7 months after AChEI initiation, age >55, male or female, any race. Memantine was allowed on stable doses between baseline and follow up MMSE. Exclusion criteria included other brain or systemic disease or medication use that could account for the cognitive impairment. All individuals who met IC/EC were enrolled.

The Texas Alzheimer Research and Care Consortium (TARCC) is a longitudinal multicentre observational study [25]. Inclusion criteria was defined as mild-moderate AD, at least 1 follow up assessment with at least 1year interval, age >55, male or female, any race and actively being treated with one of the two AChEI (donepezil, rivastigmine). Memantine was allowed as it is standard of care in moderate stage AD and was built into the statistical model. Exclusion criteria from the TARCC cohort included other brain or systemic disease or medication use that could account for the cognitive impairment. All individuals who met IC/EC were enrolled.

2.13. Statistical analysis

Experiments in the iPSC model system were performed in triplicates or quadruplicates. Values are expressed as means ± *S*.D. or ± SEM, as indicated in figure legends. Statistical significance was determined by an unpaired Student's *t*-test (two-tailed). For cumulative distribution comparison we used two-sided two sample Kolmogorov−Smirnov test. P values less than 0.05 were deemed statistically significant.

Clinical data analysis: Power calculation was not performed due to the exploratory nature of this pharmacogenetic study thus sample size was not predetermined. Significance was set at $p < 0.05$. Change in MMSE score from baseline was performed by 2-tailed T-test. The distributional assumption for the T-test was examined by QQ plot, histogram along with Shapiro-Wilk normality test. Longitudinal analysis of clinical outcome (MMSE) was performed using a fitted general linear model, based on an assumed autoregressive covariance structure. Model independent variables included age, sex, medication regimen at the time of the first utilized outcome measure (AChEI alone or AChEI plus memantine), APOE4 carrier status (0, 1 or 2 alleles as categorical variables) and CHRFAM7A genotype (carrier versus non-carrier of the functional direct allele) and interaction terms based on CHRFAM7A genotype with medication regimen and drug exposure. Type 3 test of model effects were performed in conjunction with a 0.05 nominal significance level. SAS (Cary, NC) version 9.4 statistical software was used for all analyses.

3. Results

3.1. CHRFAM7AΔ2 bp is a null allele for two Alzheimer's Disease (Ad) relevant phenotypes: α 7 nAChR channel opening and α7 nAChR mediated Aβ_{1-42} uptake

In order to define the pharmacogenetic analysis paradigm we set out to elucidate the functional role of the *CHRFAM7A* and

*CHRFAM7AΔ*2 bp alleles in two phenotypic readouts: electrophysiological studies using single channel patch-clamp on transfected Human embryonic kidney (HEK) 293 cells, and Aβ_{1-42} uptake in medial ganglionic eminence (MGE) progenitors, the precursors of basal forebrain cholinergic neurons (BFCN).

In electrophysiological studies, transfection of HEK293 cells with CHRNA7 (pcDNA3.1-CHRNA7-GFP) was used as a 0 copy model. Co-transfection of CHRNA7 with CHRFAM7A (pcDNA3.1-CHRFAM7A-GFP) (direct model) or CHRNA7 with CHRFAM7AΔ2bp (pcDNA3.1-CHRFAM7AΔ2bp-GFP) (inverted model), both in ratios 1:4, as well as transfection of CHRNA7 (0 copy model) all detected PNU 120,596 (positive allosteric modulator of α7nAChR) responsive channel opening, suggesting α7 nAChR specificity (Fig. 1a–d). The 0 copy model and the inverted model demonstrated similar activation patterns, response to PNU 120,596 and overlapping distributions of channel open probability (Fig. 1a, c, d). In contrast, CHRFAM7A transfected cells (direct model) had a decreased channel open probability, similar to the previously reported UB052 iPSC line, carrier of CHRFAM7A [11]. To aid surface expression of α7, co-transfection with intracellular chaperones Ric-3 [18] and NACHO [19] in 1:1:1 ratio was applied in all experiments.

As the α7 nAChR binds Aβ_{1-42} with high affinity, we performed genotype phenotype correlation for Aβ_{1-42} uptake. Previously, we showed that *CHRFAM7A* mitigates Aβ_{1-42} uptake, but the functional role of the *CHRFAM7AΔ*2 bp allele remained unknown. To address this question, UB068 iPSCs[11] harbouring two ancestral alleles (0 copy) were differentiated into MGE progenitors[26,14] and transfected with an empty vector, EV (pcDNA3.3-mCherry), *CHRFAM7A* (pcDNA3.1-CHRFAM7A-mCherry) and *CHRFAM7AΔ*2 bp (CHRFAM7ADelta2bp-mCherry)[17,11]. Expression of *CHRFAM7A* and *CHRFAM7AΔ*2 bp was confirmed by breakpoint specific RT-qPCR (Supplementary Fig. 1 a). Overexpression of either construct did not affect α7 nAChR expression and localization (Supplementary Fig. 1 a-d).

Concentration dependent Aβ_{1-42} uptake was quantified by flow cytometry (Fig. 1e,f) and cell counts (Fig. 1g). Fluorescent-Aβ_{1-42} uptake between concentrations of 10 nM to 250 nM demonstrated similar dose response curves in the EV and *CHRFAM7AΔ*2 bp transfected MGE progenitors (Fig. 1e - g). In contrast, *CHRFAM7A* transfected cells showed a mitigated Aβ_{1-42} uptake compared to EV beyond 50 nM ($p < 0.05$). Furthermore, ELISA revealed a significantly lower amount of Aβ_{1-42} in total cell lysate from *CHRFAM7A*

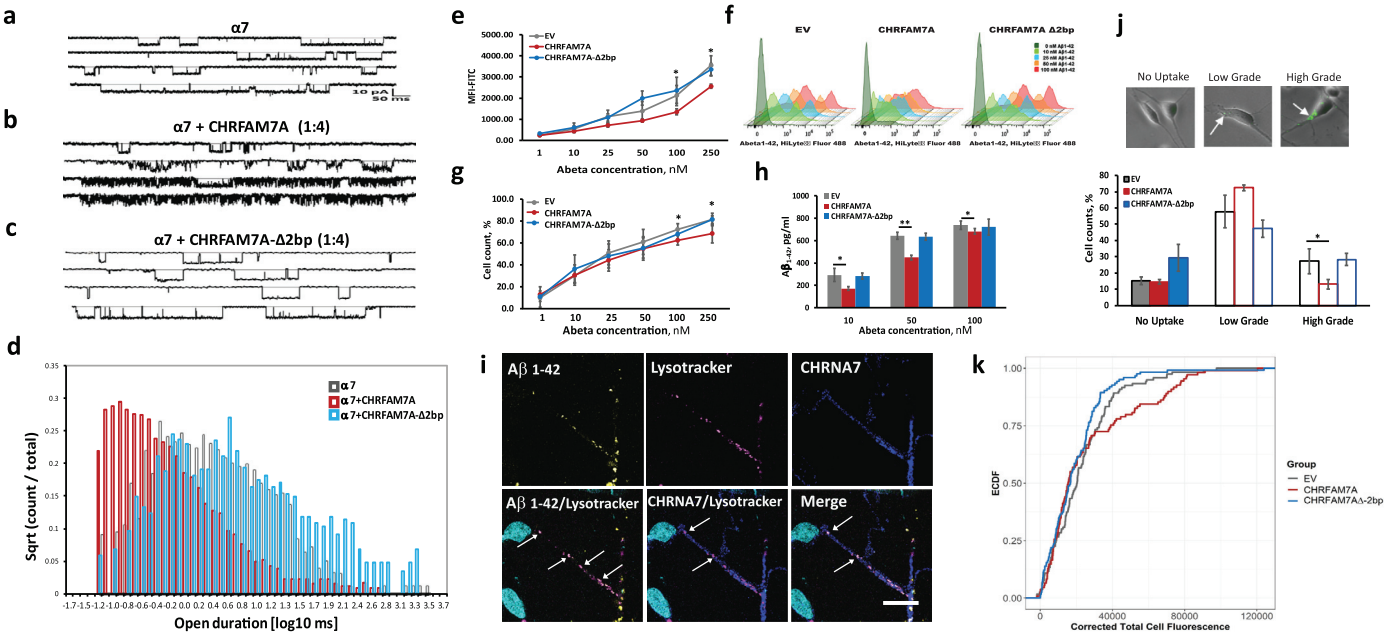

Fig. 1. Inverted CHRFAM7AD2 Bp is a null allele

Single channel traces and open dwell time for wild type α7, with or without the presence of CHRFAM7A in HEK 293 cells. Recordings were made at cell-attached patch configuration and currents were elicited by ACh and PNU 120,596, on HEK 293 cells transfected with α7nAChR alone (a), α7nAChR and CHRFAM7A direct (b); α7nAChR and CHRFAM7A inverted (c) cDNAs in 1:4. Corresponding histograms of channel open time in logarithmic time axis are shown for α7nAChR alone (gray), in the presence of CHRFAM7A (red) and CHRFAM7AΔ2bp (blue) (n = 5 from 32 independent cultures). e, Transfection of UB068 (0 copy) with *CHRFAM7A* causes a decrease in Aβ_{1-42} uptake in a concentration-dependent manner compared to transfection with empty vector (EV) analysed as mean fluorescent intensity by flow cytometry. In contrast, transfection with *CHRFAM7AΔ2bp* does not affect Aβ_{1-42} uptake via the a7nAChR. Data are presented as mean ± SD. * - $P < 0.05$ - difference between Aβ_{1-42} uptake in *CHRFAM7A* transfected cells compared to EV-transfected cells (T-test) at each given Aβ_{1-42} concentration ($n = 3$ from 3 independent cultures). f, Representative histograms of total gated events (~ 10,000 cells were analysed by flow cytometry) for median samples are presented. Gated on a uniform, normally distributed FSC-A/SSC-A population with doublet discrimination through secondary FSC-A/FSC-H analysis ($n = 3$ from 2 independent cultures). g, Overexpression of *CHRFAM7A* and *CHRFAM7AΔ2bp* in UB068 using EV as transfection control indicates that the inverted allele is a null demonstrating similar Aβ_{1-42} uptake as EV quantified by cells counts (at least 50 cells from 5 fields/condition in 4 independent cultures were counted by a blinded pathologist and two independent raters). h, Quantification of Aβ_{1-42} in total cell lysate of MGE progenitors derived from UB068 line and transfected with *CHRFAM7A, CHRFAM7AΔ2bp*, and EV constructs. The cells were incubated with indicated concentration of Aβ_{1-42} for 24 h and the amount of Aβ_{1-42} was detected by ELISA. Data are presented as mean ± SD. * - $P < 0.05$, ** - $P < 0.01$ - difference between Aβ_{1-42} uptake in *CHRFAM7A* transfected cells compared to EV-transfected cells (T-test) at each given Aβ_{1-42} concentration ($n = 3$ from 3 independent cultures). i, Representative confocal images show localization of Aβ_{1-42} (yellow), LysoTracker Deep Red (magenta), and CHRNA7 (blue) in MGE progenitors derived from UB068 line (upper panel). Nuclei were stained with DAPI (cyan). Cellular uptake of Aβ_{1-42} overlaps with LysoTracker Deep Red and CHRNA7 (lower panel). Co-localization of Aβ_{1-42} / LysoTracker and CHRNA7/LysoTracker is indicated by white arrows. Scale bar, 10 μm. The cells were incubated for 24 h with Aβ_{1-42} (100 nM), washed and incubated for an additional 5 h with LysoTrackerDeep Red ($n = 5$ from 3 independent cultures). j, Visual grading demonstrates qualitative differences in Aβ_{1-42} uptake: *CHRFAM7AΔ2bp* behaves as a null demonstrating similar Aβ_{1-42} grade distribution as EV; CHRFAM7A prevents the formation of larger Aβ_{1-42} deposits (high grade) at 100 nM of Aβ_{1-42} concentration for 24 h. Data are presented as mean ± SD. * - $P < 0.05$ - difference between high grade Aβ_{1-42} uptake in *CHRFAM7A* transfected cells compared to EV-transfected cells, T-test. Inset: representative images show low, high, and no Aβ_{1-42} uptake by MGE progenitors overexpressing *CHRFAM7A, CHRFAM7AΔ2bp* or EV (at least 50 cells from 5 fields/condition in 4 independent cultures were counted by a blinded pathologist and two independent raters). k, Grading was validated by semi-automated intensity measure using ImageJ. Distribution curves of Aβ_{1-42} uptake in MGE progenitors overexpressing *CHRFAM7A, CHRFAM7AΔ2bp* or EV are presented. Aβ_{1-42} uptake in MGE progenitors overexpressing *CHRFAM7A* was significantly lower than in those overexpressing *CHRFAM7AΔ2bp* ($P = 0.037$; two-sided p-values from two sample Kolmogorov–Smirnov test).

transfected MGE progenitors compared to the ones transfected with EV (Fig. 1h). Areas of co-localization of Aβ_{1-42} with the acidic compartment (LysoTracker) were detected by confocal microscopy consistent with lysosomal engagement (Fig. 1i). CHRNA7 expression was broader and uniform along the axons and demonstrated spots of co-localization with Aβ_{1-42} and the acidic compartment. Fluorescent Aβ_{1-42} uptake at 100 nM was qualitatively assessed and further quantified by microscopy using grading and cell counts (Fig. 1j,k). Grading was validated by semiautomatic intensity measures (Fig. 1k). Differential uptake by MGE progenitors was confirmed by a comparing cumulative intensity distribution between *CHRFAM7A* and *CHRFAM7A*Δ2 bp transfected MGE progenitors ($p = 0.037$; Kolmogorov–Smirnov test) (Fig. 1k). *CHRNA7* and *CHRFAM7A* gene expression levels were unaffected by Aβ_{1-42} treatment (Supplementary Fig. 1 e, f). While *CHRFAM7A* is an intrinsic dominant negative modulator, the inverted *CHRFAM7A*Δ2 bp functions as a null allele in regard of α7 nAChR channel opening and α7 nAChR mediated Aβ_{1-42} uptake.

3.2. Human iPSC models animal and human outcomes implicating *CHRFAM7A* as the translational gap

To study the effect of *CHRFAM7A* on drug response in the human context, we genome edited UB068 (*CHRFAM7A* null) iPSC line to express *CHRFAM7A* using TALENS mediated insertion of *CHRFAM7A* into the AVVS1 safe harbor site on 19q13.42 under the constitutively active CMV promoter (Fig. 2a). GFP was inserted in tandem under EF1a promoter to facilitate selection of successfully edited *CHRFAM7A* harbouring cells (Fig. 2b). The insertion was confirmed by PCR (Fig. 2c) and whole genome sequencing (WGS) (Supplementary Fig. 2 a, b). All lines were characterized for the expression of pluripotency markers at the gene (*NANOG, OCT3/4, SOX2*) and protein (TRA 1–60, Oct-4, Sox2) levels (Fig. 2b, Supplementary Fig. 2 c, d). Differentiation into three germ layers was assessed by the TaqMan® hPSC Scorecard™ Assay (Supplementary Fig. 2 e). WGS excluded aneuploidy, intragenic indels, and large chromosomal duplications or deletions (Supplementary Fig. 2 a, b). WGS showed a limited number of likely irrelevant *de novo* non-homonymous variants in ENST00000379458, MUC3A-201, ENST00000456556 and ANKRD36C in isogenic colony 8 and in ENST00000379458 and MUC3A-201 in isogenic colony 12 (Supplementary Tables S5 and S6). These non-homonymous changes have not been established as pathogenic. *CHRFAM7A* gene expression was consistent with the genotypes (Fig 2d). CHRFAM7A translation was confirmed by immunoblot analysis using CHRFAM7A N-terminus specific antibody (generous gift from Andrew Baird; Fig. 2e). CHRFAM7A did not alter gene expression of the α7 nAChR (Fig 2. d). The membrane localized signal detected with the loop antibody represents both CHRNA7 and CHRFAM7A proteins (Fig. 2f).

To model selective neuronal vulnerability, iPSCs were differentiated into MGE progenitors, the precursors of BFCNs and GABA interneurons[26,14]. MGE progenitors generated from UB068_CHRFAM7A line were evaluated for the presence of the specific gene and protein markers (Supplementary Fig. 3 a, b). As a nascent *CHRFAM7A* carrier, UB052 was incorporated into the panel [11]. In all three lines, fluorescent Aβ_{1-42} uptake assessed by cell counts showed genotype specific dose response curves (Fig. 2g,h). Similar results were obtained by flow cytometry (Fig. 2i). In UB068, Aβ_{1-42} uptake was linear with dose, while in UB068_CHRFAM7A and in carrier (UB052) lines mitigated Aβ_{1-42} uptake was observed (Fig. 2g–i). *CHRNA7* and *CHRFAM7A* expression remained unchanged upon dose-dependent Aβ_{1-42} uptake (Supplementary Fig.1. g, h). Neuronal toxicity measured by LDH release demonstrated congruent dose-response with Aβ_{1-42} uptake (Fig. 2j). Next, we tested the response of MGE progenitors to two FDA approved Acetylcholine Esterase Inhibitors, AChEIs (donepezil, rivastigmine) and encenicline, a selective α7 nAChR agonist. 24 h exposure to ACHEIs proved not to be toxic for the MGE cultures (Supplementary Fig. 4 a) and did not change the expression of *CHRNA7* (Supplementary Fig. 4 b). In UB068, AChEIs and encenicline decreased Aβ_{1-42} uptake (Fig. 2k), Aβ_{1-42} induced cytotoxicity measured by LDH release (Fig. 2l) and by protease activity using bis-AAF-R110 Substrate (Fig. 2m), and apoptosis measured by Caspase3/7 activity (ApoTox-Glo Triplex assay, Promega) (Fig. 2n). Furthermore, expression of apoptosis regulator *BAX* correlated with Caspase3/7 activity results (Fig. 2o). UB068 (non-carrier) is genetically equivalent to the preclinical models used in drug selection. In the *CHRFAM7A* carrier models (UB068_CHRFAM7A and UB052) neurotoxicity was unchanged by AChEIs or encenicline (Fig 2L-n), and donepezil treatment resulted in an increase in apoptosis (Fig. 2n, o). These results suggest that non-carriers of the functional direct allele should benefit from α7 nAChR targeting therapies.

3.3. Population frequency of the *CHRFAM7A* alleles

Based on the functional readouts, the population frequency of the direct, functional *CHRFAM7A* carriers and non-carriers is the key to understanding the α7 nAChR translational gap. To establish population frequencies of the dosage and alleles, we genotyped 1174 samples from the Texas Alzheimer Research and Care Consortium, Baylor College of Medicine and NCRAD (supplementary information). Genotyping of *CHRFAM7A* dosage and orientation was performed using breakpoint specific TaqMan assay to decipher copy number, and capillary sequencing to determine orientation of the alleles. Frequency of CN dosage (0, 1, 2 and 3), and alleles (ancestral, direct and inverted) are depicted in Table 1. Non-carriers of the functional direct allele comprise 25% of the human population, while carriers of the direct *CHRFAM7A* functional allele is present in 75% of the population. Normal aged controls and AD subjects have similar allele frequencies, suggesting that *CHRFAM7A* is not associated with the disease phenotype, rather it has a pharmacogenetic role for α7 nAChR targeting therapies.

3.4. *CHRFAM7A* non-carriers respond to ACHEI translating from preclinical results

Next we sought to test the α7 nAChR translational gap hypothesis in human data. Upon reviewing publicly available data on the α7 nAChR clinical trials [2,27], it became apparent that most trials were designed to test the receptor mediated cognitive enhancement as the primary outcome measure in relatively short trials of 3–6 months duration [2] and clinical trial data with DNA from the same individuals were not available. As an alternative approach, although likely less sensitive, exposure to AChEI (increasing ACh, agonist of the α7nAChR) and using *CHRFAM7A* genotype as an α7nAChR specific readout were used as a proof of principal study. Response to initiation of therapy and delayed disease modifying effect werestudied in two cohorts; the UB cohort had information on treatment initiation that was used to assess short term response, while the TARCC cohort had up to 7 years follow up that measured disease modifying treatment (DMT) effect.

For the initiation of treatment response pharmacogenetic analysis we used the UB ADMDC clinical cohort. The study fulfilled double blind criteria as at the time of assessment neither subject nor investigator was aware of the genotype. In these subjects the date of first prescription was systematically documented mimicking synchronous initiation of treatment. 63 subjects met inclusion criteria (supplementary information). 8 subjects were excluded for missing DNA sample. Demographic information is summarized in Table S3. Over 90% of the cohort was Caucasian. All subjects were on maximum doses of an AChEI, 96% on donepezil. Change in MMSE from baseline (pre-exposure) within 4–7 months of treatment initiation were compared by two-tailed T-test. Non-carriers of direct *CHRFAM7A* allele had superior response to the AChEI as predicted from the iPSC model

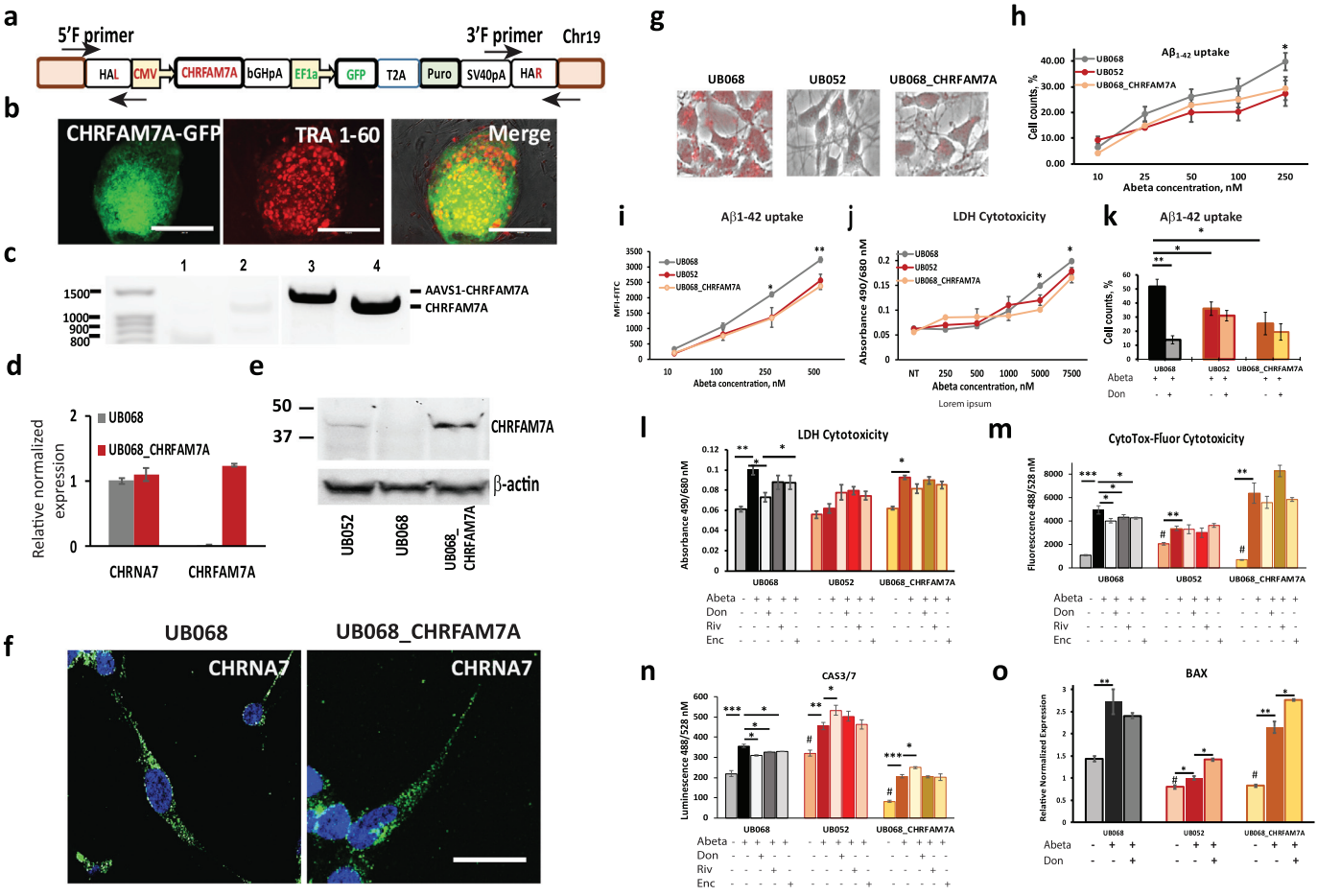

Fig. 2. Human iPSC models animal and human outcomes implicating CHRFAM7A as the translational gap

UB068 isogenic line (UB068i_CHRFAM7A) expressing *CHRFAM7A* in the AAVS1 safe harbor site. a, Schematic of the *AAVS1-CHRFAM7A* construct. 4 colonies from 2 independent electroporation experiments are being characterized. b, Representative image of TRA1−60 live staining of UB068i_CHRFAM7A line, passage 3. Scale bar, 200 μm. c, PCR verification of insertion: 1- PCR with primers for AAVS1−5′ homology arm, 2- PCR with primers for AAVS1−3′ homology arm, 3-PCR with primers spanning *AAVS1-CHRFAM7A*, 4-PCR with primers specific for CHRFAM7A d) RT-qPCR shows that overexpression of *CHRFAM7A* gene does not alter expression levels of *CHRNA7* in the genome edited line ($n = 3$ from 3 independent cultures). e) Immunoblot analysis using an antibody directed to the unique N-terminus sequence of CHRFAM7A (gift from Andrew Baird) confirms its expression in the UB068_CHRFAM7A line; positive control the previously reported UB052 *CHRFAM7A* carrier line UB052 (2 independent cultures). f) Representative confocal images demonstrate that the presence of CHRFAM7A does not affect membrane localization of CHRNA7 ($n = 10$ cells Z-stack images from 2 independent cultures). Scale bar, 10 μm. Compared to UB068, the presence of CHRFAM7A (both in UB052 and UB068_CHRFAM7A) causes a significant decrease in $A\beta_{1-42}$ uptake detected by cell counts ($n = 3$ from 3 independent cultures) (g, h) and flow cytometry (i) (Triplicates from 2 independent cultures). For h-i data are presented as mean ± SD. * - $P < 0.05$ ** - $P < 0.001$ - difference between $A\beta_{1-42}$ uptake in UB068_CHRFAM7A line compared to UB068 (T-test) at each given $A\beta_{1-42}$ concentration. $A\beta_{1-42}$-induced cytotoxicity increases in a concentration-dependent manner measured by LDH release (j) in MGE progenitors differentiated from UB068, UB068_CHRFAM7A, and UB052 lines ($n = 3$ from 3 independent cultures). Data are presented as mean ± SD. * - $P < 0.05$ - difference between $A\beta1-42$ uptake in the UB068_CHRFAM7A line compared to UB068 (T-test) at each given $A\beta1-42$ concentration. k), 24 h pre-treatment with donepezil (Don) decreases $A\beta_{1-42}$ uptake by MGE progenitors derived from UB068, but not from UB068_CHRFAM7A or UB052 lines. Data are presented as mean ± SD. * - $P < 0.05$ - difference in $A\beta_{1-42}$ uptake between the cells pre-treated with donepezil (Don, 50 μM) followed by $A\beta_{1-42}$ (250 nM, 24 h) compared to $A\beta_{1-42}$ alone. Cytotoxic effect of $A\beta_{1-42}$ (7,5 μM, 48 h) on MGE progenitors derived from the three lines was reduced by the pre-treatment with donepezil (Don), rivastigmine (Riv) and encenicline (Enc) only in UB068 line (null), while it remained unchanged in UB068_CHRFAM7A and UB052 as detected by LDH cytotoxicity assay (l), CytoTox-Glo cytotoxicity assay (m) and Caspase-Glo 3/7 assay (n). o) RT-qPCR of BAX, apoptosis activator, corresponds to the CAS3/7 readout suggesting decreased apoptosis in non-carriers compared to carrier lines (UB052, UB068_CHRFAM7A) with donepezil (Don) treatment. In the carrier lines donepezil increase BAX expression. For panels l - o data are presented as mean ± SD. * - $P < 0.05$ ** - $P < 0.001$ *** - $P < 0.0001$ - difference between non-treatment control and $A\beta_{1-42}$ and between $A\beta_{1-42}$ and drug pre-treatment. # - $P < 0.05$ - difference between non-treatment controls in UB052 and UB068_CHRFAM7A compared to UB068 (T-test). All results presented in panels l - o represent average from 4 independent experiments.

($p = 0.037$) (Fig. 3a). APOE4 carrier status had no effect (Fig. 3b). Individual level data supports the responder rates (Fig. 3c, d).

We used the TARCC longitudinal dataset to perform the DMT pharmacogenetic analysis. 345 subjects met inclusion criteria (supplementary information). Demographic information is summarized in Table S4. Over 90% of the cohort was Caucasian. 34.87% of the subjects were on maximum doses of an AChEI (mild AD) and 65.13% on AChEI and memantine at the first assessment. We used general linear model including age, sex, medication regimen at the time of visit 1 (AChEI alone or AChEI plus memantine), APOE4 carrier status (0, 1 or 2 alleles as categorical variables) and CHRFAM7A genotype (carrier versus non-carrier of the functional direct allele) and interaction terms including visit*CHRFAM7A genotype and first treatment*CHRFAM7A genotype. We found that CHRFAM7A non-carriers of the functional direct orientation allele had a statistically significant benefit from exposure to AChEI after controlling for the other variables (Fig 4a, Table 2) over the 7-year observation period. The effect was 5 points difference on the MMSE and the separation of the curves started after 3 years of follow-up. The delay in separation of the curves is likely due to the non-synchronized drug initiation. Individuals with an upslope in the first year likely were just started on an AChEI, while others were enrolled after years of drug exposure. The desynchronized drug initiation may wash out the earlier signal. However, the percentage of subjects meeting the 5-point decline cut-off at 1, 2, 3 and 4 years of follow up demonstrates the difference in carrier and non-carrier groups at those earlier time points. APOE4 carrier

Table 1
Population frequency of the CHRFAM7A dosage and alelles.

	AD ($N = 490$)		NC ($N = 657$)	
CN frequencies	N	%	N	%
0	5	0.01	6	0.01
1	98	0.20	115	0.18
2	378	0.77	526	0.80
3	9	0.02	10	0.02
Allele frequencies				
Ancestral	106	0.11	123	0.09
Direct	483	0.49	639	0.49
Inverted	391	0.40	552	0.42
Carrier frequency				
Carrier	362	0.74	476	0.73
Non-carrier	128	0.26	181	0.28

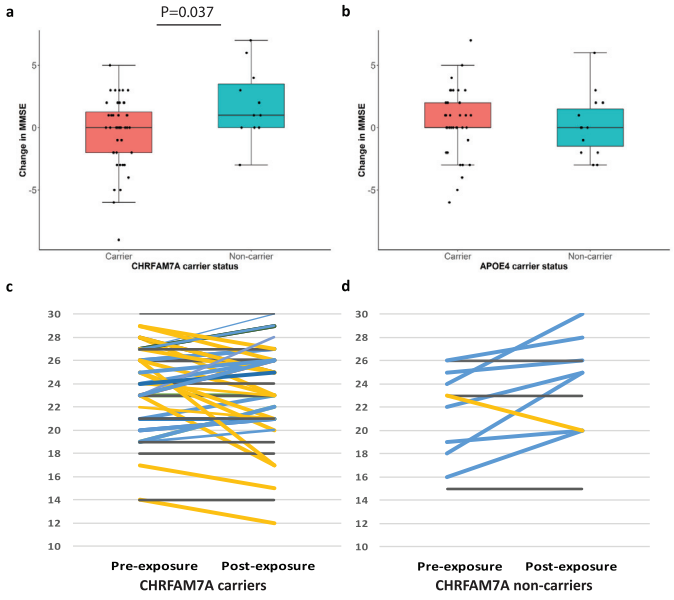

Fig. 3. CHRFAM7A non-carriers have a superior response to first exposure of AChEI
Pre- and post-exposure double blind pharmacogenetic study using MMSE as primary outcome measure. Response to initiation of ChEI therapy in 55 subjects. (a) CHRFAM7A non-carriers demonstrate superior response to first exposure when compared to carriers ($p = 0.037$; two-tailed T-test). (b) APOE4 carrier status does not affect first exposure response to AChEIs. Individual level pre- and post-exposure data in CHRFAM7A carriers (c) and non-carriers (d).

status (0, 1 or 2 alleles) did not demonstrate a treatment response effect (Fig 4b). Individual level data and demographics are shown in Fig. 4c, d and Table S4. CHRFAM7A carriers had minimal benefit if any compared to the natural history of AD cognitive decline. The non-carrier individuals demonstrate the outcome predicted from preclinical data. These data suggest a disease modifying effect in a genotype specific manner.

4. Discussion

The α7 nAChR has been a promising target for diseases affecting cognition and higher cortical functions; however, the effect observed in animal models failed to translate into human clinical trials identifying a translational gap. *CHRFAM7A* is a human specific fusion gene between *CHRNA7* and *FAM7A/ULK4*, and as it is not present in any other species the *CHRFAM7A* effect was not accounted for in preclinical studies. We hypothesized that *CHRFAM7A* may account for this translational gap and understanding its function may offer novel approaches to explore α7 nAChR as a drug target in a genotype specific manner. From previous experimental and in *silico* work the inverted allele was predicted to be non-translated, thus non-functional [7]. To experimentally validate the prediction, we performed functional characterization of the inverted and direct alleles using two disease relevant phenotypes, electrophysiology and Aβ_{1-42} uptake with associated neuronal toxicity using iPSC model. *CHRFAM7A*Δ2 bp allele behaved as a functional null for channel function, while *CHRFAM7A* decreased channel open time indicating dominant negative effect. In the presence of *CHRFAM7A* allele, Aβ_{1-42} uptake was mitigated at post-physiological levels [11] while *CHRFAM7A*Δ2 bp showed similar dose response as the null line. Both neuronal toxicity and Aβ_{1-42} uptake were dose-dependent and were mitigated by *CHRFAM7A*, but not by *CHRFAM7A*Δ2 bp. The null alleles (ancestral and inverted) are equivalent to the preclinical animal models.

To study the effect of *CHRFAM7A* on drug response in the human context, we used a panel of iPSC lines including non-carrier (UB068), nascent CHRFAM7A carrier (UB052); and we genome edited UB068 (*CHRFAM7A* null) iPSC line to express *CHRFAM7A* for isogenic control. To model selective neuronal vulnerability, iPSCs were differentiated into MGE progenitors, the precursors of BFCNs and GABA interneurons [26,14]. In UB068, Aβ_{1-42} uptake was linear with dose, while in UB068_CHRFAM7A and in carrier (UB052) lines Aβ_{1-42} uptake was mitigated. Parallel to uptake, similar dose response was detected for cytotoxicity measured by LDH release. AChEIs and encenicline, an α7 nAChR agonist, demonstrated a beneficial effect on Aβ_{1-42}-induced cytotoxicity in the non-carrier line in contrast with the carrier lines. Change in apoptosis appeared to be the driving cell death mechanism for the detected difference. To establish population frequencies of the alleles, we genotyped 1147 samples using breakpoint specific TaqMan assay to decipher copy number, and capillary sequencing to determine orientation of the alleles. Locus specific genotyping is required to detect *CHRFAM7A* as the only unique sequence is the breakpoint sequence. The inversion is even more challenging to detect in general, however, in this case the Δ2 bp deletion allows a high throughput assay. These two characteristics, being a fusion gene and the inversion event, make *CHRFAM7A* elusive on SNP and CNV microarrays and even WGS underperforms due to miss-mapping of the short reads. Locus specific genotyping using sensitive technology and functional characterization established that non-carriers of *CHRFAM7A* compose 25% of the population in Caucasians, similar to responder rates in AChEI clinical trials [28]. As preclinical development is carried out largely in nonhuman models, drugs screened for α7 nAChR as a target, without accounting for *CHRFAM7A,* will likely benefit only 25% of the population; for the 75% we need models that harbor CHRFAM7A. The 25%–75% split washes out the effect in the 25%. Previous genotyping efforts reported markedly different allele frequencies [8,29] in African-American, Caucasian and Hispanic populations suggesting that clinical trial admixture, or lack of it, may also affect efficacy readouts.

As α7 nAChR clinical trial data with DNA samples were not available, we used exposure to AChEI (increasing ACh, an agonist of the α7 nAChR) and *CHRFAM7A* genotype as an α7 nAChR specific readout as a proof of principal study. We performed double-blind pharmacogenetic analysis on the effect of AChEI therapy based on *CHRFAM7A* carrier status in two paradigms: response to drug initiation and DMT effect. Both paradigms demonstrated the benefit for the CHRFAM7A non-carriers consistent with the prediction. In the DMT analysis to align with the clinical trials that led to FDA approval of the three AChEI drugs, we included mild-moderate AD subjects. According to practice standards, the majority of subjects were on maximum doses of an AChEI (mild AD) or AChEI and memantine (moderate AD) and continued on the same regimen throughout the study or memantine was added when moderate stage was reached. We found that as predicted, CHRFAM7A non-carriers of the functional direct orientation allele had a statistically significant benefit from exposure to AChEI after controlling for the other variables. Of note, the study is double

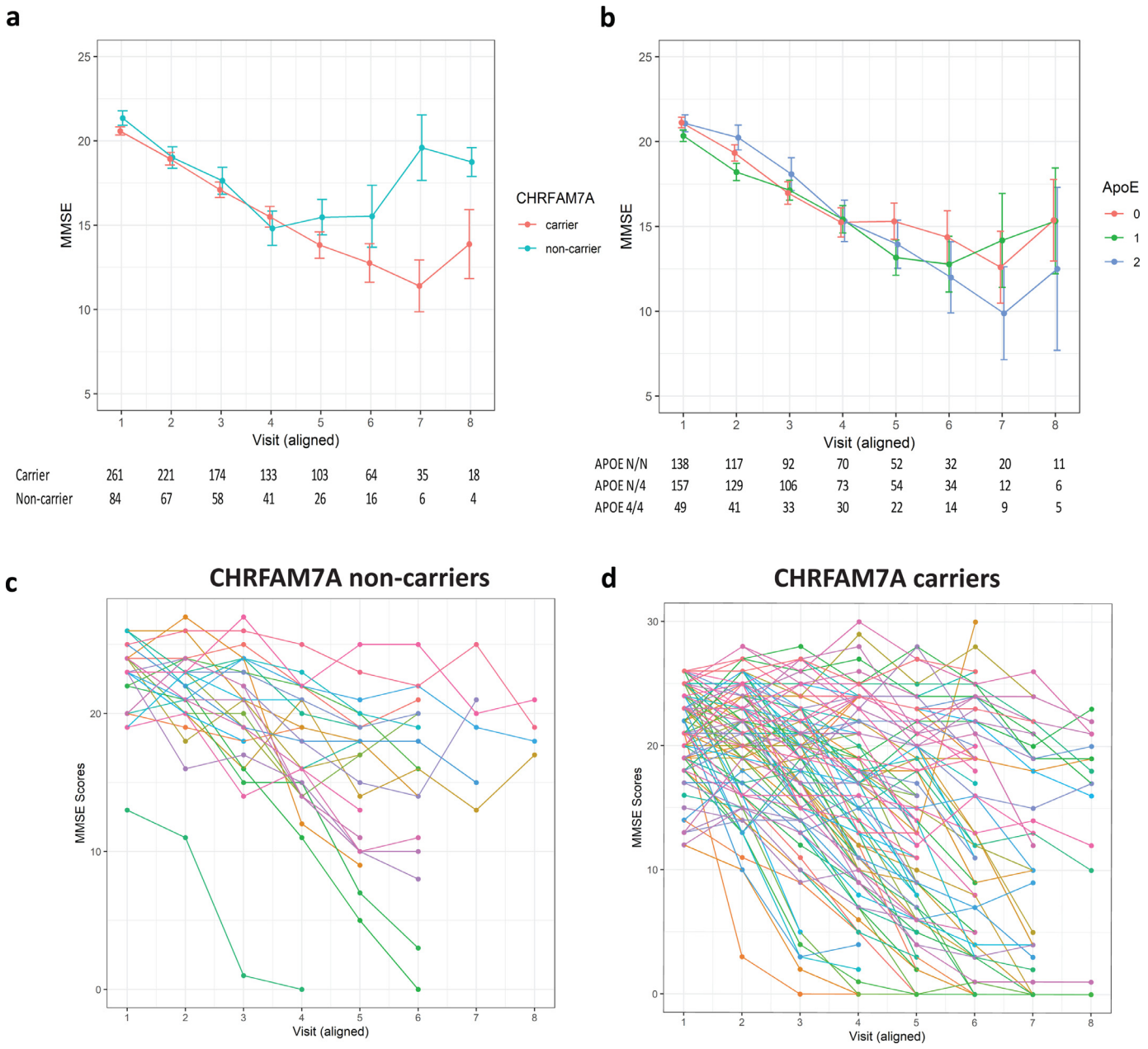

Fig. 4. CHRFAM7A non-carriers have a DMT benefit from AChEI

Longitudinal double blind pharmacogenetic study using MMSE as primary outcome measure demonstrating DMT effect in the TARCC cohort over a 6-year observation period ($p = 0.0048$). Mean plot shows the mean MMSE scores across all visits grouped by CHRFAM7A genotype (a) and by number of APOE4 alleles (b). Attrition is depicted below the curves. Individual profile plots demonstrate the MMSE score for each individual across all visits in CHRFAM7A non-carries (c) and carriers (d).

blind as neither subjects nor rater had knowledge of the genotype at the time of assessments. The attrition rate is high; however, it is expected in a study of this length in this vulnerable population.

Table 2
Type 3 Tests of Fixed Effects for MMSE as outcome.

Effect	Num DF	Den DF	F Value	Pr > F
visit	7	805	49.08	<0.0001
age	1	298	4.78	0.0295
gender	1	298	7.84	0.0054
CHRFAM7A	1	298	8.08	0.0048
ApoE	2	298	1.25	0.2868
firsttrt	1	298	16.96	<0.0001
*CHRFAM7A*visit*	7	805	2.23	0.0304
*CHRFAM7A*firsttrt*	1	298	0.54	0.4611

CHRFAM7A carriers had minimal benefit, if any, compared to the natural history of AD cognitive decline. These findings suggest that CHRFAM7A may account for the translational gap in α7 nAChR, and more broadly cholinergic therapies. The non-carrier individuals demonstrate the outcome predicted from preclinical data and the frequency of the non-carriers in the AD population is consistent with the responder rates from the AChEI trials. CHRFAM7A carriers likely require different small molecules screened in a model that harbours CHRFAM7A.

Mechanistic insights from the *in vitro* work suggests competitive binding between ACh and $A\beta_{1-42}$ to the α7 nAChR as both agonist and antagonist mitigates $A\beta$ uptake. The α7 nAChR binds $A\beta$ with high affinity [30] and internalizes $A\beta$ into the endosomes/lysosomes and mitochondria [31,32]. Uptake of $A\beta$ phosphorylates p38, induces apoptosis [31] and α7 nAChR agonists mitigate the $A\beta$-induced

apoptosis in animal models [33]. Further studies are needed to elucidate the mechanistic link between receptor structure and Aβ binding with specifically designed studies incorporating genetic and pharmacological paradigms.

While the presented work is focusing on receptor function, another possible mechanism needs to be considered: the control of neuroinflammation by donepezil through the cholinergic anti-inflammatory pathway. The clinical readout is from chronic drug exposure, which raises the possibility of upregulation of CHRNA7 as demonstrated in rat models after long-term exposure to donepezil, 4 days [34,35]. Interestingly, donepezil treatment decreases LPS induced neuroinflammation in rats [36]. These data suggest that donepezil has an anti-inflammatory effect by upregulating CHRNA7 and, as a result, enhancing the α7 nAChR mediated cholinergic anti-inflammatory pathway. In humans, the presence of CHRFAM7A refines the neuroinflammatory response. In human primary macrophages, donepezil upregulates both CHRNA7 and CHRFAM7A which likely increases the anti-inflammatory tone [12]. While upon LPS stimulation CHRFAM7A is downregulated [37], concomitant donepezil and LPS exposure synergistically upregulates CHRNA7 and extinguishes the opposite effects on CHRFAM7A [12]. As a result, in the absence of stimulation by Pathogen-associated molecular pattern molecules (PAMPs) and perhaps Damage-associated molecular patterns (DAMPs) an anti-inflammatory milieu is set by donepezil [12] . Once an immune trigger in present, such as LPS or Aβ, CHRFAM7A refines the inflammatory tone to activate the innate immune response [11,36]. These immune regulatory differences between rat (non-carriers of CHRFAM7A) and humans (studied lines are CHRFAM7A carriers) could account for the DMT effect in non-carriers by controlling Aβ (DAMP) triggered neuroinflammation.

While randomized, double blind, placebo controlled studies are needed, these findings have several important implications. First, this is the first proof of concept study that genotype and mechanism specific treatment is feasible in AD. Second, CHRFAM7A non-carriers, 25% of the AD population accounting for approximately 1.5 million people with AD in the US could benefit from α7 nAChR selective drugs. Several compounds have been extensively studied in phase 1 and 2 clinical trials with valuable data to support and accelerate α7 nAChR targeting drug development. Those efforts need to be continued with trial design incorporating *CHRFAM7A* pharmacogenetics. Third, FDA approved AD drugs (AChEIs) may have a DMT effect in non-carriers and need to be tested in preclinical AD and aMCI. Fourth, 75% of patients have an intrinsic modulator for α7 nAChR, thus compounds need to be screened for this group in the relevant model harbouring *CHRFAM7A*. Fifth, agents that reduce amyloid burden could be more effective in non-carriers as the same Aβ dose reduction has a larger effect based on the uptake and toxicity dose response-curves. The vast amount clinical data on amyloid reducing agents, including monoclonal antibodies and BACE inhibitors, should be reanalysed based on this concept, as they may have had an effect in 25% of patients.

There are several limitations to our study that invite caution and further work. The clinical studies presented build on observational cohorts, however they do fulfill the double-blind criteria as assessments were performed prior to genotyping thus both subjects and raters were blind to the genotype. Although placebo was not used in its traditional sense, the predicted lack of efficacy in the *CHRFAM7A* carriers serves as a predefined comparison group. Attrition rate was high in the DMT study, inviting for caution, although the individual plots do not suggest a systemic effect. The delay in the observed difference could be the results of non-synchronous initiation of therapy, as prior to the time of enrolment subjects were treated for variable periods of time. This non-synchronous start of drug exposure likely reduces power thus works against the findings. The clinical data needs validation in additional datasets and placebo controlled, randomized, double blind studies are needed to detect the DMT effect of α7 nAChR targeting drugs, and more broadly cholinergic strategies. Furthermore, the preclinical iPSC model is from a limited number of representative individual for carriers and non-carriers. A larger panel of iPSC is needed to serve as model system for small molecular screen with population relevance.

Although much work is needed, these observations open new opportunities to explore completed clinical trials. For example, post hoc reanalysis of the AChEI trials in aMCI based on *CHRFAM7A* carrier status could detect a signal in the non-carriers in delaying conversion, thus offer an early disease modifying effect. In addition, as CHRFAM7A non-carriers have an Aβ_{1-42} dose-dependent neuronal vulnerability they are most likely to benefit from Aβ_{1-42} reduction, thus post hoc reanalysis of the plethora of anti-amyloid therapies may in fact find an effective agent for 25% of AD. For the 75% of carriers, we need relevant preclinical models to screen compounds and basic science to understand the impact of CHRFAM7A on AD pathogenesis. This pharmacogenetic paradigm may apply to other treatment strategies targeting α7 nAChR.

Declaration of interests

The authors declare no conflict of interest.

Author contributions

K.S. conceptualized and designed the study, both the laboratory experiments and clinical aspects, led the wet lab experimental design and data interpretation, performed the first exposure pharmacogenetic study and wrote the first draft of the manuscript. I.I. performed the iPSC experiments, contributed to data interpretation and worked extensively on the manuscript. B.B. contributed the genome editing of the iPSC line. Z.C. performed the statistical analysis for both pharmacogenetic studies. A.O. contributed with scoring in the wet lab experiments and ascertaining the UB clinical cohort. D.I.V performed the patch clamp experiments and contributed the electrophysiological sections of the manuscript. L.C. performed data capture and analysis of the flow cytometry experiment, and wrote those sections in the manuscript. N.S. developed the grading system and was the blinded pathologist for scoring and contributed those sections of the manuscript. J.S.R. performed the data management and extraction from the longitudinal TARCC database. V.P. contributed to the clinical data of the TARCC cohort and participated in the clinical data analysis. R.H.B. contributed clinical data collection, neuropsychological review of the UB cohort and revised the manuscript. A.A. designed the electrophysiological experiments and contributed to those sections of the manuscript. G.W. designed and managed the clinical data analysis for both pharmacogenetic studies and contributed those sections to the manuscript.

Acknowledgements

This study was made possible in part by the Texas Alzheimer's Research Consortium (TARCC) funded by the state of Texas through the Texas Council on Alzheimer's Disease and Related Disorders. This work was supported by Alzheimer Association AARG-16–443615, Edward A. and Stephanie E. Fial Fund, Community Foundation for Greater Buffalo.

NCRAD receives government support under a cooperative agreement grant (U24 AG21886) awarded by the National Institute on Aging (NIA). We thank contributors who collected samples used in this study, as well as patients and their families, whose help and participation made this work possible. The funding agencies had no role in study design, data collection, data analysis, interpretation or writing of the report.

Supplementary materials

Supplementary material associated with this article can be found, in the online version, at doi:10.1016/j.ebiom.2020.102892.

References

[1] Bertrand D, Lee C-HL, Flood D, Marger F, Donnelly-Roberts D. Therapeutic Potential of α7 Nicotinic Acetylcholine Receptors. Pharmacol Rev 2015;67(4):1025.

[2] Yang T, Xiao T, Sun Q, Wang K. The current agonists and positive allosteric modulators of α7 nAChR for CNS indications in clinical trials. Acta Pharm Sin B 2017;7(6):611–22.

[3] Thomsen MS, Hansen HH, Timmerman DB, Mikkelsen JD. Cognitive improvement by activation of alpha7 nicotinic acetylcholine receptors: from animal models to human pathophysiology. Curr Pharm Des 2010;16(3):323–43.

[4] Gault J, Robinson M, Berger R, Drebing C, Logel J, Hopkins J, et al. Genomic organization and partial duplication of the human alpha7 neuronal nicotinic acetylcholine receptor gene (CHRNA7). Genomics 1998;52(2):173–85.

[5] Araud T, Graw S, Berger R, Lee M, Neveu E, Bertrand D, et al. The chimeric gene CHRFAM7A, a partial duplication of the CHRNA7 gene, is a dominant negative regulator of alpha7*nAChR function. Biochem Pharmacol 2011;82(8):904–14.

[6] de Lucas-Cerrillo AM, Maldifassi MC, Arnalich F, Renart J, Atienza G, Serantes R, et al. Function of partially duplicated human alpha77 nicotinic receptor subunit CHRFAM7A gene: potential implications for the cholinergic anti-inflammatory response. J Biol Chem 2011;286(1):594–606.

[7] Sinkus ML, Graw S, Freedman R, Ross RG, Lester HA, Leonard S. The human CHRNA7 and CHRFAM7A genes: a review of the genetics, regulation, and function. Neuropharmacology 2015;96(Pt B):274–88.

[8] Sinkus ML, Lee MJ, Gault J, Logel J, Short M, Freedman R, et al. A 2-base pair deletion polymorphism in the partial duplication of the alpha7 nicotinic acetylcholine gene (CHRFAM7A) on chromosome 15q14 is associated with schizophrenia. Brain Res 2009;1291:1–11.

[9] Lasala M, Corradi J, Bruzzone A, Esandi MDC, Bouzat C. A human-specific, truncated alpha7 nicotinic receptor subunit assembles with full-length alpha7 and forms functional receptors with different stoichiometries. J Biol Chem 2018;293(27):10707–17.

[10] Wang Y, Xiao C, Indersmitten T, Freedman R, Leonard S, Lester HA. The duplicated α7 subunits assemble and form functional nicotinic receptors with the full-length α7. J Biol Chem 2014.

[11] Ihnatovych I, Nayak TK, Ouf A, Sule N, Birkaya B, Chaves L, et al. iPSC model of CHRFAM7A effect on α7 nicotinic acetylcholine receptor function in the human context. Transl Psychiatry 2019;9(1):59.

[12] Maroli A, Di Lascio S, Drufuca L, Cardani S, Setten E, Locati M, et al. Effect of donepezil on the expression and responsiveness to LPS of CHRNA7 and CHRFAM7A in macrophages: a possible link to the cholinergic anti-inflammatory pathway. J Neuroimmunol 2019;332:155–66.

[13] Liu Y, Liu H, Sauvey C, Yao L, Zarnowska ED, Zhang S-C. Directed differentiation of forebrain GABA interneurons from human pluripotent stem cells. Nat Protoc 2013;8:1670.

[14] Ihnatovych I, Lew A, Lazar E, Sheng A, Kellermayer T, Szigeti K. Timing of Wnt Inhibition Modulates Directed Differentiation of Medial Ganglionic Eminence Progenitors from Human Pluripotent Stem Cells. Stem Cells Int 2018;2018:3983090.

[15] Wang Y, Xiao C, Indersmitten T, Freedman R, Leonard S, Lester HA. The duplicated alpha7 subunits assemble and form functional nicotinic receptors with the full-length alpha7. J Biol Chem 2014;289(38):26451–63.

[16] Warren L, Manos PD, Ahfeldt T, Loh YH, Li H, Lau F, et al. Highly efficient reprogramming to pluripotency and directed differentiation of human cells with synthetic modified mRNA. Cell Stem Cell 2010;7(5):618–30.

[17] Ma Y, Jin J, Dong C, Cheng E-C, Lin H, Huang Y, et al. High-efficiency siRNA-based gene knockdown in human embryonic stem cells. RNA (New York, NY) 2010;16(12):2564–9.

[18] Williams ME, Burton B, Urrutia A, Shcherbatko A, Chavez-Noriega LE, Cohen CJ, et al. Ric-3 promotes functional expression of the nicotinic acetylcholine receptor alpha7 subunit in mammalian cells. J Biol Chem 2005;280(2):1257–63.

[19] Matta JA, Gu S, Davini WB, Lord B, Siuda ER, Harrington AW, et al. NACHO Mediates Nicotinic Acetylcholine Receptor Function throughout the Brain. Cell Rep 2017;19(4):688–96.

[20] Nayak TK, Purohit PG, Auerbach A. The intrinsic energy of the gating isomerization of a neuromuscular acetylcholine receptor channel. J Gen Physiol 2012;139(5):349–58.

[21] Milescu LS, Nicolai C, Yildiz A, Selvin PR, Sachs F. Hidden Markov model applications in QuB: analysis of nanometer steps in single molecule fluorescence data and ensemble ion channel kinetics. Biophys J 2003;84(2) 124a-a.

[22] Hu X, Crick SL, Bu G, Frieden C, Pappu RV, Lee JM. Amyloid seeds formed by cellular uptake, concentration, and aggregation of the amyloid-beta peptide. Proc Natl Acad Sci U S A 2009;106(48):20324–9.

[23] Woodward MR, Amrutkar CV, Shah HC, Benedict RH, Rajakrishnan S, Doody RS, et al. Validation of olfactory deficit as a biomarker of Alzheimer disease. Neurol Clin Pract 2017;7(1):5–14.

[24] Woodward MR, Hafeez MU, Qi Q, Riaz A, Benedict RHB, Yan L, et al. Odorant Item Specific Olfactory Identification Deficit May Differentiate Alzheimer Disease From Aging. Am J Geriatr Psychiatry 2018;26(8):835–46.

[25] O'Bryant SE, Waring SC, Cullum CM, Hall J, Lacritz L, Massman PJ, et al. Staging Dementia Using Clinical Dementia Rating Scale Sum of Boxes Scores: a Texas Alzheimer's Research Consortium Study. JAMA Neurol 2008;65(8):1091–5.

[26] Liu Y, Liu H, Sauvey C, Yao L, Zarnowska ED, Zhang SC. Directed differentiation of forebrain GABA interneurons from human pluripotent stem cells. Nat Protoc 2013;8(9):1670–9.

[27] Lewis AS, van Schalkwyk GI, Bloch MH. Alpha-7 nicotinic agonists for cognitive deficits in neuropsychiatric disorders: a translational meta-analysis of rodent and human studies. Prog. Neuropsychopharmacol. Biol. Psychiatry 2017;75:45–53.

[28] Burns A, Yeates A, Akintade L, Del Valle M, Zhang RY, Schwam EM, et al. Defining treatment response to donepezil in Alzheimer's disease: responder analysis of patient-level data from randomized, placebo-controlled studies. Drugs Aging 2008;25(8):707–14.

[29] Kunii Y, Zhang W, Xu Q, Hyde TM, McFadden W, Shin JH, et al. CHRNA7 and CHRFAM7A mRNAs: co-localized and their expression levels altered in the postmortem dorsolateral prefrontal cortex in major psychiatric disorders. Am J Psychiatry 2015;172(11):1122–30.

[30] Wang HY, Lee DH, D'Andrea MR, Peterson PA, Shank RP, Reitz AB. beta-Amyloid (1-42) binds to alpha7 nicotinic acetylcholine receptor with high affinity. Implications for Alzheimer's disease pathology. J Biol Chem. 2000;275(8):5626–32.

[31] Ma KG, Lv J, Yang WN, Chang KW, Hu XD, Shi LL, et al. The p38 mitogen activated protein kinase regulates beta-amyloid protein internalization through the alpha7 nicotinic acetylcholine receptor in mouse brain. Brain Res Bull 2018;137:41–52.

[32] Wang HY, Li W, Benedetti NJ, Lee DH. Alpha 7 nicotinic acetylcholine receptors mediate beta-amyloid peptide-induced tau protein phosphorylation. J Biol Chem 2003;278(34):31547–53.

[33] Chang KW, Zong HF, Ma KG, Zhai WY, Yang WN, Hu XD, et al. Activation of alpha7 nicotinic acetylcholine receptor alleviates Abeta1-42-induced neurotoxicity via downregulation of p38 and JNK MAPK signaling pathways. Neurochem Int 2018;120:238–50.

[34] Akaike A, Takada-Takatori Y, Kume T, Izumi Y. Mechanisms of neuroprotective effects of nicotine and acetylcholinesterase inhibitors: role of alpha4 and alpha7 receptors in neuroprotection. J Mol Neurosci 2010;40(1–2):211–6.

[35] Takada-Takatori Y, Kume T, Ohgi Y, Fujii T, Niidome T, Sugimoto H, et al. Mechanisms of alpha7-nicotinic receptor up-regulation and sensitization to donepezil induced by chronic donepezil treatment. Eur J Pharmacol 2008;590(1–3):150–6.

[36] Tyagi E, Agrawal R, Nath C, Shukla R. Cholinergic protection via alpha7 nicotinic acetylcholine receptors and PI3K-Akt pathway in LPS-induced neuroinflammation. Neurochem Int 2010;56(1):135–42.

[37] Benfante R, Antonini RA, De Pizzol M, Gotti C, Clementi F, Locati M, et al. Expression of the alpha7 nAChR subunit duplicate form (CHRFAM7A) is down-regulated in the monocytic cell line THP-1 on treatment with LPS. J Neuroimmunol 2011;230(1–2):74–84.